Fiber Laser Micro-machining of Ti-6Al-4V

A. Sen, B. Doloi and B. Bhattacharyya

Abstract Progress of laser micro-machining i.e. micro-cutting, micro-drilling, Micro-channeling, micro-grooving, micro-turning etc. in the field of aeronautic, automobile, semiconductor and biomedical industries such as turbine blades of aircraft engine, automotive fuel filters, combustion chambers, surgical needles and micro-fluidic devices have emerged extensively in the present era. The prime contributor to the success of laser micro-machining in the recent years is fiber laser technology that involves the combination of diode pumped solid state lasers and fiber technology. This is the most promising substitute to the high-power, bulk solid-state lasers and some gas lasers owing to its simplicity, ruggedness, cost effectiveness, low maintenance, higher efficiency, higher reliability and smaller spot size. Fiber lasers are mainly characterized by short pulse lengths which range from millisecond to picosecond and even femtosecond for precise micro-machining of different materials. Titanium alloys play crucial roles in the areas of advanced structures and technologies for aerospace and power industry, medicine, automatics and mechatronics and various measurement equipments, because of their high strength and stiffness at elevated temperatures, high corrosion resistance, fatigue resistance, high strength to weight ratio and ability to withstand moderately high temperatures without creeping. The conventional machining methods intended for cutting these alloys not only suffer due to poor thermal conductivity, low elastic modulus and high chemical affinity at elevated temperatures but also have to undergo higher cost associated with the machining of Ti-6Al-4V caused by lower cutting speeds and shorter tool life. Numerous research works have been conducted with laser beam micro-machining approaches on titanium alloys mainly on Ti-6Al-4V, in order to establish the optimal experimental conditions that are to be used in different applications. However, the physical mechanism which leads to the

A. Sen (✉) · B. Doloi · B. Bhattacharyya
Production Engineering Department, Jadavpur University, Kolkata 700032, India
e-mail: abhishek.sen1986@gmail.com

B. Doloi
e-mail: bdoloionline@rediffmail.com

B. Bhattacharyya
e-mail: bb13@rediffmail.com

S.N. Joshi and U.S. Dixit (eds.), *Lasers Based Manufacturing*,
Topics in Mining, Metallurgy and Materials Engineering,
DOI 10.1007/978-81-322-2352-8_15

observed geometry and surface roughness of the micro-machined surface is still behind the veil. The aim of the present chapter is to make an in depth study of the fiber laser micro-grooving of Ti-6Al-4V, discussing vividly the fiber laser machining system, the occurring physical processes and machining strategy and influence of various process parameters. Experimental results of present research work along with the work of various researchers are discussed so as to validate and run down hypotheses on the mechanisms involved.

Keywords Micro-machining · Fiber laser · Ti-6Al-4V alloy · Micro-grooving process

1 Introduction

Laser micro-machining process includes wide range of versatile processes which deals with the removal of stringent amount of molten material in the range of microns (Scientific Technical Committee of the Physical and Chemical Machining Processes of CIRP, 1–500 μm was adopted as the range for micro-machining work) (Masuzawa and Tonshoff 1997). In general other related manufacturing processes such as micro-joining and micro-adjustment (Meijer 2002) by the laser beam can also be termed as micro-machining process. Generally, the micro-machining term is broadly classified into the ablation, micro-cutting, micro-drilling, marking in the ranges of micron. This chapter aims to focus on the aspect of micro-grooving (broadly micro-machining i.e. micro-cutting) of titanium alloys of grade 5 (Ti-6Al-4V) by fiber laser machining system. The average power of various laser systems that are identified to be best suitable for micro-machining applications of wide range of engineering materials are 20–50 W. In brief, laser micro-machining is mainly characterized by a machining process in which small amount of material is removed by focusing highly intense laser beam on the work-piece surface as the generated heat from the laser beam melts and then vaporizes the work-piece throughout the thickness of the material (Meijer 2002). The molten material can be expelled from the cutting front by a pressurized assist gas jet that includes compressed air pressure, inert gaseous systems i.e. argon, helium, nitrogen and sometimes enhanced material removal can also be conducted through chemical reactions such as oxidation of the material (Sun and Brandt 2013).

Progress in engineering in the field of advanced structures and technologies for aerospace and power industry, biomedical, automatics and mechatronics, manufacturing of control and measurement equipment, is driven to a large extent by development and application of new or modified functional materials. It includes titanium and its alloys, although initially they were intended mainly for applications in structural material to carry loads and carrying airframe elements for aerospace industries. Titanium alloy of grade 5 enables implementation of new solutions in

structures and technologies and orthopaedics for its unique properties such as low cytotoxicity and biocompatibility (Ratner et al.1996), corrosion resistance (Hayes and Mow 1997), wear resistance (Chesnutt et al. 1980) and fatigue resistance (Collings 1984; Williams 1984; Fasasi et al. 2009). In most applications, Ti-6Al-4V implants have relied on surface roughening and porous coatings to improve osseointegration (Fasasi et al. 2009). The potential for micro-parts as medical tools operating at cellular level is increasing which drives extensive research efforts to be concentrated on the evolution and control of the titanium alloys microstructure through the adjustment of the processing parameters in order to obtain desirable balance of properties for specific applications. The challenges in understanding the mechanisms involving machining of titanium alloys along with its low thermal conductivity (laser beam machining process) and the high tool wear associated with the reactivity of titanium with tool materials (traditional machining process) are still to be addressed.

Fiber lasers evolved as the most versatile and rapid growing laser systems during the last decade and successfully emerged into the various fields of manufacturing, medical, metrological and military applications that were previously dominated by conventional solid state lasers and gas lasers. Today, fiber lasers (average power of 10–50 W) hold a good market share in the domain of fine and precise micro-cutting that involves the combination of both continuous mode and pulse mode with the aid of fusion cutting (inert gas) to sublimation cutting (oxygen cutting). The initiation of combining optical fiber with laser system was started when the advantages of introducing a rare earth doped single-mode optical fiber in a laser cavity to provide a robust single spatial mode at the laser output was recognized in 1961 by Snitzer (1961). After a few years, high gain in neodymium-doped multimode silica optical fiber lasers pumped by flash lamps was demonstrated by Snitzer and Koester (1964). In the mid-1980s, practical work on single-mode optical fiber lasers commenced, after the initial advancement of rare-earth-doping methods that used modern optical fiber fabrication processes based on vapor-phase deposition technique (Hegarty et al. 1983; Nakazawa et al. 1989; Poole et al. 1985). For the majority of the 1990s, the highest-power single-mode optical Fiber lasers were usually pumped either by gas lasers or solid-state lasers, which turned out to be irrelevant in case of commercial, industrial applications owing to low average power drawn from most single-mode fiber lasers (Teodoro 2011). Finally, the booming of the telecommunications during 2001 caused the thrust needed for the development of high-power optical fiber lasers. Extensive amount of dedicated research works and development of multimode pump diodes brought about significantly more powerful and reliable multimode pump diodes at radically lower cost. It is worth noting that the contribution of the Military-funded programs, in a drive for directed energy weapon system and countermeasures which was another driving force for higher powers from fiber lasers and the development of related technologies (Hecht 2009).

1.1 Advantages of Fiber Lasers Over Other Solid State and Gas Lasers

Shorter wavelength in combination with its high focus ability, better system flexibility, high component yield, long uptime along with improved reliability, high repeatability, high aspect ratios with utmost precision, unlimited material coverage, low cost and fully automated processes seem be advantageous for fiber lasers in thin sheet metal cutting. Whereas, the CO_2 lasers are probably still capable of machining thicker materials more efficiently. Although, Olsen et al. (2009) study revealed efficiency of fiber laser cutting operation for thick materials is higher than of CO_2 laser. Their experimental results also revealed that burr free cuts can be achieved in 1 and 2 mm AISI 304 stainless steel, over a wide range of cutting rates using multi-beam fiber laser machining system. Further research studies in the domain of fiber laser machining process also brought about the observations that fiber lasers can produce better results as compare to CO_2 lasers when machining of copper and magnesium alloys. Fiber lasers have also been replacing Nd-YAG lasers in various micro-machining applications such as micro-cutting of stents, thin sheet of ferrous and non-metals in terms of cutting speed, cut edge quality and the length of micro cracks. Fiber laser cutting of thick polycrystalline silicon (silicon wafer) is another significant area where it produces better results compared to Nd-YAG laser. The fundamental wavelengths of fiber lasers lie between 1 and 2 μm (Schaeffer 2012) and can couple extremely well with wide range of metals. The long thin gain media of fiber lasers produce high quality beams which are focussed to a very small spot on the work piece surface, giving very high power density. The high efficiency of the laser diodes produce considerably high wall plug efficiency compared to other conventional lasers. Other important characteristics of fiber lasers have active regions of several kilometres long which can provide kilowatt levels of continuous output power. Fiber lasers are also benefited due to flexible coupling of the light with the fiber for which light can be delivered easily to a movable focusing element. Efficient cooling can be achieved because of long fiber length that leads to high surface to volume ratio. High vibrational stability, extended lifetime and maintenance free operation (Schaeffer 2012) appears to be advantageous and results into more compactness in the case of fiber laser system as compared to other conventional solid state and gas lasers. Therefore, in the present scenario, fiber lasers are outpacing market growths mainly in the areas of automotive, aerospace, wind turbines, solar processing and bio-medical devices.

1.2 Need of Laser Beam Micro-grooving Process

Micro-grooves are used as one of the key micro-features in different micro-products like micro-thermal devices, micro-heat exchangers, micro-reactors, micro-pumps and micro-mechanical systems. A high aspect ratio micro-groove not only provides

a large surface area for heat dissipation and reaction systems but also provides high capillary force for micro-heat pipes and micro-pumps, as micro-fluidics, frictional force and capillarity vary according to the geometry of the micro-groove (Rathod et al. 2013). Micro-grooves can also be used as micro-channels in biomedical and biochemical applications such as super alloys, titanium alloys, aluminium alloys, copper alloys etc., which are hard and difficult to cut by conventional machining methods. The effectiveness of the laser micro-grooving process mechanism depends on the thermal properties and the optical properties to a certain extent. Mechanical properties of the materials that are to be machined do not play significant roles as compare to other mentioned properties. Energy transfer between the laser and the material occurs through irradiation for which no cutting forces are generated by the laser. As a consequence, mechanically induced material damage, tools wear and machine vibrations cannot be observed. Moreover, the material removal rate (MRR) for laser machining is not limited by constraints such as maximum tool force, built-up edge formation or tool chatter. In order to obtain fine and deep micro-grooves i.e. grooves with high aspect ratio (width/depth), importance of different properties such as reflectivity, thermal conductivity, specific heat and latent heats of melting and evaporation is crucial.

1.3 Importance of Ti-6Al-4V Micro-grooves in Research and Industrial Perspective

Ti-6Al-4V is the most used material out of the other titanium alloys and its total production is almost half of all titanium alloys. The present research work is dedicated towards the bio-medical features of this alloy, giving priority to both the geometrical aspects i.e. width and depth and surface topology i.e. surface roughness at the time of selecting the process parameters. Titanium alloys (grade 5) are often used in different bio-medical field of applications such as artificial hip joints, knee joint replacements and also dental implants. It is important that Ti-6Al-4V can bond firmly with the bones, for optimal function and durability. Therefore, enhanced bioactivity and improved implant-host interactions are important so as to reduce biological related implant failure. The process of osseointegration mainly depends upon the various surface properties such as surface chemistry, surface topography, surface roughness and the surface energy. Modified improved surfaces confer enhancement of cell-implant interactions and brings about more opportunities for focal attachment which are beneficial for orthopaedic applications (Brown and Arnold 2010). Therefore, selection of optimum machining parametric conditions holds the key behind obtaining precise micro-grooves with minimum surface roughness. Thereafter, these precise and fine micro-grooves can be optimized to integrate with the surrounding tissue.

1.4 Basic Mechanism of Laser Micro-grooving Process of Ti-6Al-4V

Most of the titanium alloys that are used in the industry contain α- and β- stabilizers which include Ti-6Al-4V, Ti-6Al-6V-2Sn and Ti-6Al-2Sn-4Zr-6Mo. The chemical compositions of Ti-6Al-4V are listed in table 1. These alloys are heat treatable and most are weldable especially with the lower β-stabilizer (Sieniawski et al. 2013). According to Ezugwu et al. (2003), machinability can be defined as the difficulty to machine a particular material under a given set of the machining parameters such as cutting speed, feed rate and depth of cut. Conventional machining process fails to meet stringent quality control at the time of machining of titanium alloys owing to excessive amount of heat, work hardening, low thermal conductivity, abrasiveness and high strength level. In contrast, laser beam machining is fast and repeatable process. The heat generated during the laser beam machining process, is used to remove material in a very small volume without mechanical engagement with work-piece material. The basic mechanism involved behind laser beam micro-grooving process can be identified as the laser beam micro-cutting process includes several crucial factors. During laser beam micro-machining of titanium alloy of grade 5, temperature zones can be divided into solidus temperature of 1877 K, liquidus temperature of 1923 K and evaporation temperature of 3533 K. Four different approaches which govern laser beam machining process are evaporative laser cutting, fusion cutting, reactive fusion cutting and controlled fracture technique. The selection of optimum laser cutting technique depends on the thermo-physical properties of the material, the thickness of the work piece and the type of laser employed. For a thick section cutting of titanium alloy, the most preferred process is reactive fusion cutting. In reactive fusion cutting, molten material is removed and the lost material is compensated by further melting of the work-piece at the solid-liquid interface below the cutting front (Mahrle and Beyer 2009). The present topic covers fiber laser micro-machining of Ti-6Al-4V having thickness of 1.1 mm. It is worth to take a note that all the research experiments were carried out in atmospheric conditions.

Fiber laser beam is focused on the surface of Ti-6Al-4V and some portion of the energy (optical energy is converted to heat energy) is absorbed. Theoretically, only 40–80 % of that energy may be absorbed in most cases of fiber lasers. Remaining part of the energy is reflected back and some portions of the energy may be scattered through the work-piece. Absorption occurs through a very thin surface layer and the absorbed energy diffuses into bulk of the material. As the pulse width in the present system is in nanosecond pulse regime, the heat flow can be assumed to be one dimensional (Meijer 2002). The absorbed laser beam penetrates on the

Table 1 Chemical composition of Ti-6Al-4V

Al (%)	Fe (%)	C (%)	N (%)	O (%)	V (%)	Ti
5.55–6.5	<0.25	<0.08	<0.05	<0.2	3.35–4.5	Balance

work-piece surface in the range of microns and sub microns. As the temperature increases, surface temperature will reach to the melting point at a certain period of time. The melting time reduces drastically when power density increases rapidly. Another important aspect that should be taken into consideration is that all the experiments were accomplished in pulse mode and thus the peak power is high at a considerable amount which can cause high vaporization rate. The high vaporization rate can create a shock wave and a high vapour pressure at the liquid surface considerably increases the boiling temperature (Meijer 2002). Finally the molten material is removed as vapour by the expulsion of melt, as the resultant of the high pressure in combination with super heated liquid after the end of the laser pulse. As all the research experiments were carried out in atmospheric conditions, heat affected zone (HAZ) and re-solidification of the material may occur in a form of rim (Meijer 2002). Overall laser beam micro-machining process of Ti-6Al-4V including representation of laser beam process of micro-groove generation is shown in Fig. 1 (a) & (b) respectively.

1.5 Literature Review on Laser Beam Micro-machining of Ti-6Al-4V

In the previous sub-chapter, various research aspects of Ti-6Al-4V were discussed and the difficulties of major issues of machining of these alloys were also addressed. Researchers studied laser beam micro-machining (LBMM) and laser assisted micro-machining (LAMM) approaches with different combinations of assist gas pressure system so as to optimize the various process parameters depending upon the applications. Ti-6Al-4V grooves can be machined in water and silicon oil conditions but formation of bubbles and cracks are obvious in such machining conditions. These cracks can be formed on the surface of the liquid-machined grooves because of the induced additional thermal stresses from the rapid quenching. This sub-chapter not only focuses on the various research works on laser beam micro-machining of Ti-6Al-4V that enhances bone healing and implant integration but also on various other research works related to laser beam micro-grooving process.

The mechanisms involved laser beam micro-grooving process that can be compared to micro-cutting process, except for the evacuation of scoria in the range of microns, which cannot flow out in the rear side of the micro-grooved surface as is realized in a micro-cut surface. Al-Hajri et al. (2005) studied the characterization of copper-finned micro-grooved surfaces for effective evaporation heat transfer, which can be applied to cooling of high flux electronics. Mauclair et al. (2013) reported cross sectional profile of micro-grooves machined in stainless steel by ultrafast laser machining system. They relied on spatial beam shaping technique in which the intensity distribution was utilized for precisely controlling of the pulse overlapping during the translation of the sample under femtosecond exposure. Experimental results revealed a good agreement with the priori calculations based on the ablation rate and pulse overlapping. Dhupal et al. (2008) investigated pulsed Nd:YAG

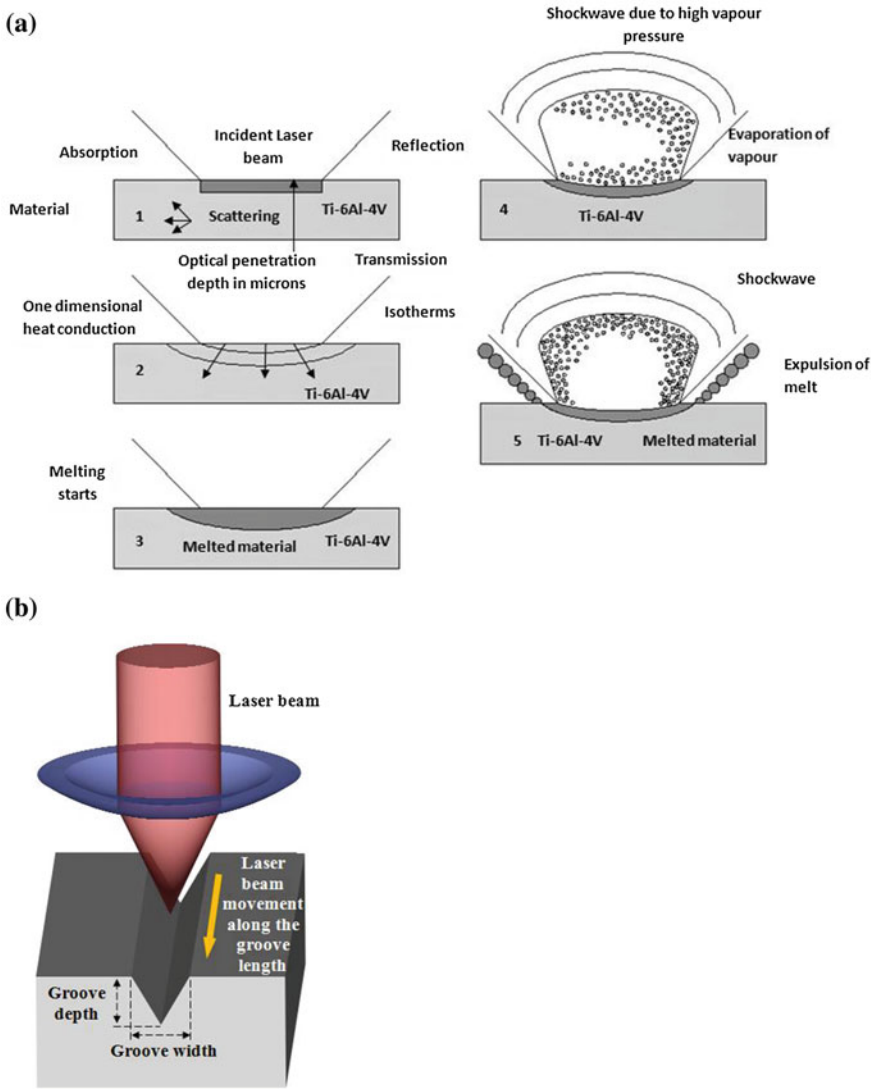

Fig. 1 **a** Representation of laser beam micro-machining of Ti-6Al-4V. **b** Representation of laser beam process of micro-groove generation in terms of width and depth

laser-turning operation to generate micro-groove on cylindrical work-piece of aluminum oxide ceramic material. They concluded that minimum depth deviation can be achieved by moderate settings of the lamp current with moderately high pulse frequency.

Various research efforts have been concentrated on improving the bone-implant interface, with the aid of either physical or chemical approaches. The physical

approach is focused on the modification of the implant surface morphology and topography using mechanical methods such as machining, acid-etching, plasma spraying, grit-blasting and anodization in order to improve the micro-topography of the surface. Increase in surface roughness of the implant material would provide a higher level of surface energy which would improve bone anchorage, matrix protein adsorption, osteoblasts functions and ultimately osseointegration (Wang and Poh 2013). The most preferred assist gas system which involves the inert gasses nitrogen, argon and helium was found out. In contrast, when this alloy is cut with oxygen assist gas at even low pressure, the uncontrolled burning of cutting front starts, which results into wide kerf width and poor surface quality. At the time of air assisted laser cutting, the reaction of titanium with oxygen and nitrogen produces a thin layer of hard and brittle oxides and nitrides and also generates much thicker HAZ in comparison to that of argon (Zhang et al. (2007). Therefore, it was suggested that, in order to overcome these problems titanium alloys may be cut using inert gasses such as argon and helium. Chen et al. (2009) studied the effects of nano-second pulse UV laser multi scale laser texturing on Ti-6Al-4V substrate on the adhesion of osteoblast cells. The researchers found that groove width was not significantly affected either by the number of passes or the distance between pulses. The effect of pulse energy on groove width was critical. In contrast, groove depth was affected by the translation distance and the number of passes as well as laser pulse energy. They also reported that laser processing conditions also affect surface roughness and other sub-micron features created on the surface. Almeida et al. (2006) performed a factorial designed experimentation on Nd: YAG laser cutting of Ti and Ti alloy sheets. It was concluded that use of nitrogen assist gas increases surface hardness from 2 to 3 times due to the formation of titanium nitride (TiN) while a mixture of He and Ar gases reduce the irregular edges and also eliminate the nitride formation. It was also reported that micro-milling of titanium alloy for medical applications especially for implants can create free-form surfaces, which lead to improvement in biocompatibility. Therefore, in order to produce functional micro-products, not only part features and tolerances have to be concerned but also surface quality must be considered as well. Several approaches have been used in order to gain a control over the surface finish of micro-features; for example, process parameters optimization, surface generation modelling and simulation, effects of using lubrication etc. Sun et al. (2008) performed laser assisted machining trials on commercially pure (alpha) titanium alloy and observed significant reductions in the cutting forces due to laser pre-heating and smoother surface finish due to the diminished fluctuations in the cutting forces. Similarly, Dandekar et al. (2010) observed an increase in tool life up to a cutting speed of 107 m/min during laser assisted turning of Ti-6Al-4V alloy. Sun et al. (2011) also carried out laser assisted milling trials on Ti-6Al-4V alloy and reported a dramatic reduction in the feed force and the tool edge chipping which is the dominant tool failure mode in dry milling of this alloy. Shelton and Shin (2010b) conducted a study of LAMM slotting of Ti-6Al-4V stainless steels AISI 422 (422SS) and AISI 316 (316SS) with tungsten carbide (WC) micro end mills. Fasasi et al. (2009) showcased the effects of nano-second laser-processing parameters i.e. pulse repetition rate, scan speed and wavelength on micro-groove geometry. To fabricate micro-structure having approximately 11 μm width and depth, Ti-6Al-4V

plate of 6 mm × 6 mm × 12 mm was utilized with Q-switched nanosecond laser. The researchers successfully demonstrated the laser ablated micro-grooves without cracks. Desired 8–12 μm micro-groove depths and widths could be achieved by controlling pulse frequency, scan speed and lens focal length that controls spot size. Shelton and Shin (2010a) again studied LAMM side cutting experiments of 316SS, 422SS, Ti-6Al-4V and Inconel 718 (IN718) of fin work-piece structure. Experimental results revealed that formation of burrs in Ti-6Al-4V and IN718 were drastically reduced with the aid of laser-assist machining (Rashid et 2012). Yang et al. (2010) developed a 3D finite element model so as to predict the formation of HAZ during laser-assisted milling of Ti-6Al-4V. They developed a proper correlation between the predicted HAZ and measurements. A transient, 3D finite volume prismatic thermal model was also developed by the researchers' group for laser-assisted milling (Tian et al. 2008). The thermal model was then utilized for the modeling of the temperature field during LAMM processes of different configurations. This prismatic thermal model provided the transient temperature distributions within the work-piece and validated through surface temperature measurements using an infrared camera and embedded thermocouples.

2 Working Principle of Fiber Laser Generation

The working principle of fiber laser can be identified with the production of laser light that requires material (a rare earth element) in the active medium which is to be raised from its ground state to an excited state (population inversion) in that medium. Normally atoms in the active medium reside in their ground states and some external form of energy must be added to raise these atoms to an excited state. Laser is generated when the laser diodes are pumped to excite lower energy molecules to excited states. The number of laser diodes depends on the application of the fiber laser and the output power required. Laser is generated by 'spontaneous emission' and then amplified by 'stimulated emission' along the axis of the resonator cavity. Inside the fiber, generated light propagates in the mode form. Mode of travel along the axis of the waveguide is constant with its characteristic propagation and group velocity. It is important that light which incidents on the boundary between fiber core and cladding, should be at angles greater than critical angle and must undergo a total internal reflection (Teodoro 2011). Light rays are guided through the core without refraction into cladding. The cavity mirrors consist of two primary optics, front and rear mirror; reflect the photons to and fro through the laser medium to increase amplification. Through the pumping process, only a fraction of energy passes through the front mirror. In conventional fibers doped single-mode core and a cladding, the laser power is restricted to about 1 W. To achieve higher output powers, fiber lasers use double-clad fibers as the amplifying medium (Schaeffer 2012). Most of fiber lasers employ Q switch mode of operation though

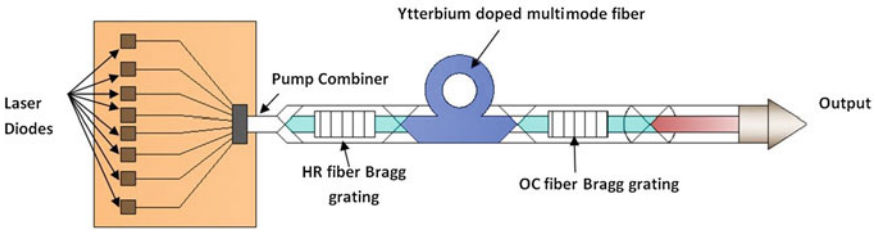

Fig. 2 Simple schematic diagram of Q switched ytterbium doped fiber laser

introduction of 'master oscillator, power amplifier' (MOPA) design enables independent control of pulse width, pulse repetition frequency and average power. End-to-end all-fusion-spliced-fiber MOPA designs, is a very common design for the use of fiber-coupled semiconductor laser. In Q switched fiber laser systems, pulse energy is independent of the fiber length. A simple schematic diagram of Q switched ytterbium doped fiber laser is shown in Fig. 2.

3 Experimental Studies on Fiber Laser Micro-machining of Ti-6Al-4V

Details of fiber laser micro-machine setup, along with the experimental plan and results have been thoroughly discussed in this chapter.

3.1 Fiber Laser Micro-machining Setup

The key elements of fiber laser are (a) optical fiber, (b) rare earth dopant ions, (c) mirrors, (d) pump sources and (e) fiber coupler. Laser interaction with the optical fiber material is dependent on several parameters i.e. laser source (wavelength and emission regime, mainly) and also on the characteristics of the material itself. Optical fiber (main component) is a cylindrical dielectric waveguide made of low-loss material such as a silica glass. The improvement of the optical properties is accomplished by doping with ytterbium (Yb^{3+}), neodium (Nd^{3+}) as rare earth elements. Yb^{3+} holds several advantages compared to other rare earth elements owing to a longer upper-state lifetime, a small quantum defect (results in lower thermal load per unit of pump power) and absence of the excited state absorption. To create laser cavity, various types of mirrors can be used in fiber lasers, i.e. bragg gratings, multilayer dielectric mirrors or semiconductor saturable absorber mirrors (SESAM) (Schaeffer 2012). In most of the cases, pumping is done predominantly by semiconductor diode lasers. Different semiconductor materials are used for different wavelengths such as aluminum gallium arsenide lasers, output ranging

from 750 to 950 nm. The output of the diode laser is directly injected into the laser fiber. In order to increase the pump power reaching to the fiber, multiple diode lasers are used. Fiber couplers are being used either one side of input fibers or one side of output fibers so that the emitted light cannot go back towards the source.

In the present research, all the experiments were carried out on multi-diodes pumped Ytterbium (Yb^{3+}) doped fiber laser machining system of 50 W, made by M/S Sahajanand Laser Technology Limited. Total 8 number of laser diodes are used for pumping and each of the diodes is coupled with the multimode of optical fibers. The photographic view of the fiber laser machining system along with diode pointer and F-θ lens (shown separately) were used in the present research work as represented in Fig. 3a, b respectively. The laser head of the fiber laser consists of both electric and galvanometer unit from which the generated laser beam is focused on the work piece with the aid of F-θ lens of 100 mm. The mode of operation in which experiments were carried out was Q switched mode which can generate a high level of peak power in the regime of kilowatts. The present experimental setup is also boosted by nanosecond pulse regime for which material interaction time with the laser beam is less. The diode pointer assures that the work piece is on the focal plane. The work-piece remains stationary and the laser beam moves to and fro to the programmed directions (by software) and highly focused generated beam is directed to the work-piece. The detailed machining setup is listed in Table 2.

3.2 Experimental Planing

Due to the complexity of relationship between laser-cutting parameters and the cutting quality, four process parameters i.e. scan speed, pulse frequency, average power and number of pass were considered so as to find out the influence of fiber laser micro-grooving process parameters on various responses such as width, depth and surface roughness. The objective of the present research work was to study the minimization of width and surface roughness and maximization of the depth although the present research work exclusively deals with the basic experimental studies. Extensive pilot experiments were carried out previously so that all the desired results could be achieved. Another important objective was to fabricate micro-grooves with utmost precision and improved surface roughness in atmospheric conditions. The literature review revealed that only few works have been carried out in such conditions and the end results regarding surface quality were not satisfactory. The present research work was also important for narrowing the gap between the theoretical and experimental studies. After the micro-machining, the samples were cleaned with the ultrasonic cleaner for 15 min so as to remove dust particles. The dimensions of the depth and width were measured using Leica optical microscope using 5× lens. The measurements of the widths were taken inside four/five (depending upon the width dimensions' variation) different places of the micro-grooves and the final width was calculated on the basis of average of four/five values. The measurements of the depth were carried out from the surface edges of

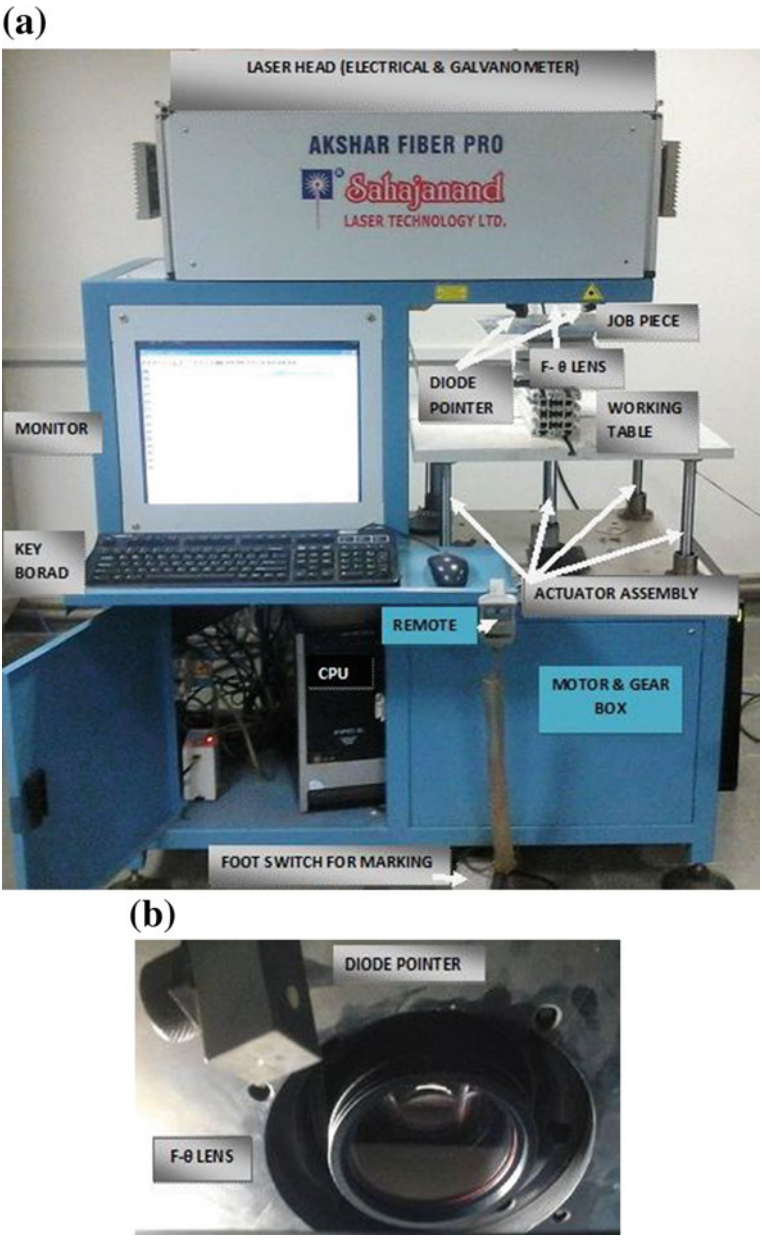

Fig. 3 **a** Photographic view of fiber laser machining system. **b** Photographic view of lens and diode pointer (Courtesy of Sahajanand Laser Technology Limited)

Table 2 Specification of the fiber laser

No.	Specification	Description
1	Laser type	Pulsed
2	Wavelength	1064 nm
3	Mode of operation	Pulsed
4	Mode of laser beam	TEM_{00}
5	Beam diameter	8.8–9 mm
6	Laser beam spot diameter	18–20 μm (after focus)
7	Average power	50 W
8	Pulse width	120 ns
9	Pulse repetition rate	50–120 kHz
10	Output fiber length	3 m

the sample material. Surface roughness (R_a) of the micro-grooves was computed by atomic force microscope (Nanosurf Easy Scan 2). The surface topology measurements were carried out by a small probe placed at the tip of a cantilever beam and the forward scanning were done from the left to right of the selected surface of the work-piece. All the measurements of the surface roughness using AFM are conducted by line fit which calculates the first order least squares fit (mean value and slope) for each line of data points and subtracts the fitted values from the raw measurement data for each data point of that line. The 3D view of the surface topology and measured surface roughness values of each groove in terms with R_a were utilized to analyze and validate the micro-grooving process. Origin 8 (data analysis and graphing software) was utilized for parametric plots with the measured values of width, depth and R_a so as to identify effects of the process parameters for the understanding of fiber laser micro-machining process for fabricating the micro-grooves on Ti-6Al-4V.

3.3 Experimental Results and Discussions

The results of the total 49 experiments consist of four set of experiments which include diferent level of micro-cutting parameters. The results of the total 49 experiments are listed in Table 3.

3.4 Influence of Process Parameters on Micro-groove Geometry and Surface Roughness

In this present sub-section, influence of four process parameters on the micro-groove geometry and surface roughness have been explained in detail.

Table 3 Results of the total 49 experiments

Ex.	Number of passes	Scan speed (mm/s)	Pulse frequency (kHz)	Average power (W)	Width (μm)	Depth (μm)	R_a (μm)
1	8	1000	80	30	145.852	113.701	0.419
2	8	900	80	30	144.451	198.033	0.450
3	8	800	80	30	124.645	112.285	0.210
4	8	700	80	30	155.512	144.958	0.145
5	8	600	80	30	149.855	136.230	0.130
6	8	500	80	30	171.548	164.612	0.103
7	8	400	80	30	174.580	175.964	0.180
8	8	300	80	30	169.541	349.098	0.209
9	8	200	80	30	224.72	367.372	0.109
10	8	100	80	30	197.638	515.670	0.044
11	8	90	80	30	220.689	387.885	0.205
12	8	80	80	30	207.658	415.315	0.505
13	8	70	80	30	205.693	415.258	0.511
14	8	60	80	30	213.668	401.594	0.245
15	8	50	80	30	232.772	481.512	0.236
16	8	40	80	30	232.772	454.673	0.115
17	8	30	80	30	236.893	481.868	0.179
18	8	20	80	30	188.611	613.832	0.212
19	8	10	80	30	186.274	750.829	0.100
20	8	05	80	30	321.385	748.923	0.169
21	8	40	50	30	319.007	821.558	0.087
22	8	40	60	30	351.115	880.702	0.263
23	8	40	70	30	349.805	839.754	0.108
24	8	40	80	30	375.595	791.742	0.213
25	8	40	90	30	350.871	803.632	0.119
26	8	40	100	30	340.456	746.961	0.118
27	1	40	50	30	279.094	759.799	0.130
28	2	40	50	30	279.094	812.343	0.140
29	3	40	50	30	340.464	812.019	0.169
30	4	40	50	30	324.245	824.667	0.237
31	5	40	50	30	246.853	862.59	0.228
32	6	40	50	30	247.779	867.667	0.140
33	7	40	50	30	262.206	905.615	0.137
34	8	40	50	30	261.834	779.146	0.151
35	9	40	50	30	249.980	747.445	0.167
36	10	40	50	30	238.465	755.312	0.262
37	11	40	50	30	235.065	735.082	0.276
38	12	40	50	30	234.118	738.054	0.277
42	5	100	50	2.5	320.017	475.500	0.198

(continued)

Table 3 (continued)

Ex.	Number of passes	Scan speed (mm/s)	Pulse frequency (kHz)	Average power (W)	Width (μm)	Depth (μm)	R_a (μm)
43	5	100	50	5	373.093	479.653	0.272
44	5	100	50	7.5	379.653	473.043	0.286
45	5	100	50	10	384.777	559.074	0.329
46	5	30	100	7.5	124.133	516.072	0.026
47	5	30	100	10	111.292	198.064	0.051
48	5	30	100	12.5	106.327	32.982	0.064
49	5	30	100	15	150.159	49.038	0.100

3.4.1 Influence of Scan Speed on Width, Depth and Surface Roughness on Ti-6Al-4V Micro-grooves

Previous research articles revealed that the fiber lasers are more effective in cutting operations than the conventional CO_2 lasers because of their linear energy per unit sheet thickness. Fiber lasers are capable of producing high energy intensity to cause the work-piece vaporization and create a keyhole owing to shorter wavelengths (Dahotre and Harimkar 2008). The cutting quality is mainly governed by the combination effects of pulse frequency and scan speed. In pulse mode of laser micro-machining operation, the extent of spot overlapping determines the surface roughness of the micro-groove geometries. During pulsed fiber laser micro-grooving operation of titanium alloys, minimization of surface roughness, width as well as increase in dimensions of depth of the micro-groove criterion is most important for various fields of engineering applications. Another important concerning factor is the formation of heat affected zone that can have a detrimental effect on the surface roughness of the fabricated micro-groove geometry. To overcome this phenomenon to a large extent, many of the experiments were carried out with higher scan speed in the moderate setting of pulse frequency with the combination of other process parameters that were kept as constants.

Figure 4 shows the influence of scan speed on width, depth and surface roughness on fiber laser machined micro-groove surfaces while other process parameters were kept constant such as 8 number of passes, pulse frequency of 80 kHz and average power of 30 W. Increase in scan speed causes the energy density to decrease and less amount of heat to be conducted to the work-piece resulting in reduction in thickness of HAZ layers. As mentioned previously, if the spot overlapping increases then the surface roughness will tend to decrease. It is worth mentioning that in this present 20 set of experiments, pulse frequency was set at moderately low value, but pulse width was relatively at high value. When scan speed was at lower value, it produced high level of spot overlapping and continuous power density per unit length. On the other hand, when scan speed was increased at moderate setting of pulse frequency, it produced low spot overlapping, discontinuous power density and less material interaction time. Due to continuous power

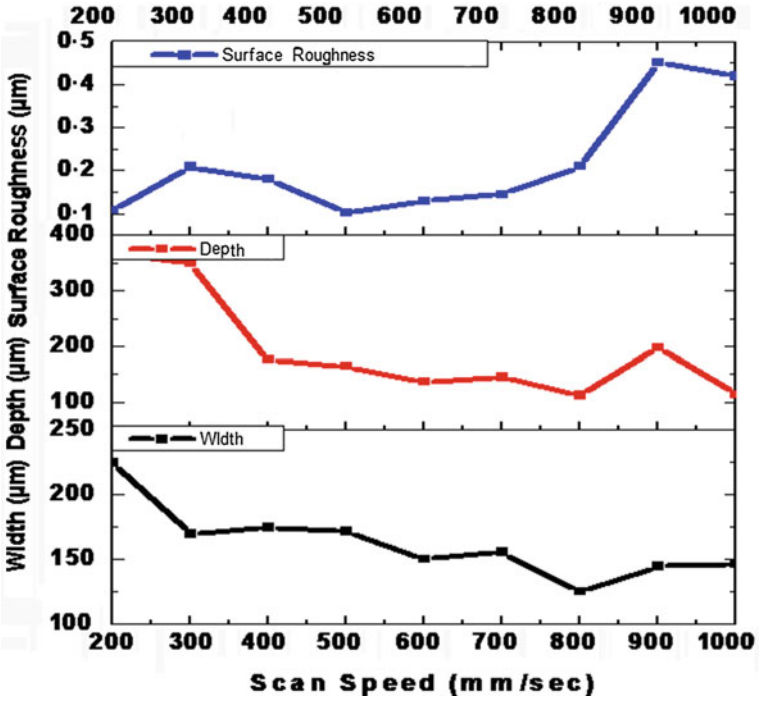

Fig. 4 Effect of scan speed on width, depth and surface roughness

density and more spot overlapping produced by lower scan speeds, dimensions of both width and depth were more as compared to the phenomenon observed at higher scan speed. In addition to that, reduction of penetration rate at each pass and sputtering of molten materials were observed at the micro-groove surfaces because of high number of passes. Each mentioned parameters had pivotal roles on Ti-6Al-4V micro-groove geometry and surface topology. Therefore, variations in both width and depth dimensions were observed at high scan speed and both had the tendency to reduce. In contrast, surface of Ti-6Al-4V micro-grooves showed reverse results for the same reasons. As a result, surface of the machined micro-grooves became rough at higher scan speed and vice versa.

3.4.2 Influence of Pulse Frequency on Width, Depth and Surface Roughness on Ti-6Al-4V Micro-grooves

Pulse mode operation of the fiber laser system provides a high instantaneous power for a period of pulse duration and followed with a period of power off. During pulse mode fiber laser micro-grooving operation, melt ejection occurs in each laser pulse

during the time when melt front cools during pulse off-time. It is important for the micro-grooving operation to reduce the quantity of the dross formation which can be achieved by producing low heat input. The relationship between pulse frequency, laser beam energy and average power is shown by Eq. 1. Low heat input can also reduce the quantity of melt formed but also imparted sufficient cooling between two successive laser pulses which prevented overheating of the cut front (Steen and Mazumder 2010).

Figure 5 shows the influence of pulse frequency on width, depth and surface roughness of fiber laser machined micro-groove surfaces while other process parameters were kept constant such as 8 number of passes, scan speed of 40 mm/s and average power of 30 W. It can be observed in the present set of experiments that scan speed remained constant at a moderately high value. This was beneficial not only for understanding the complex phenomenon of pulse frequency on the micro-groove geometry but also for reducing the surface roughness in a considerable amount. Equation 1 revealed that pulse frequency varies inversely with the laser beam energy when laser average power is constant. Therefore, when pulse frequency was increased during the present set of experiments, keeping other

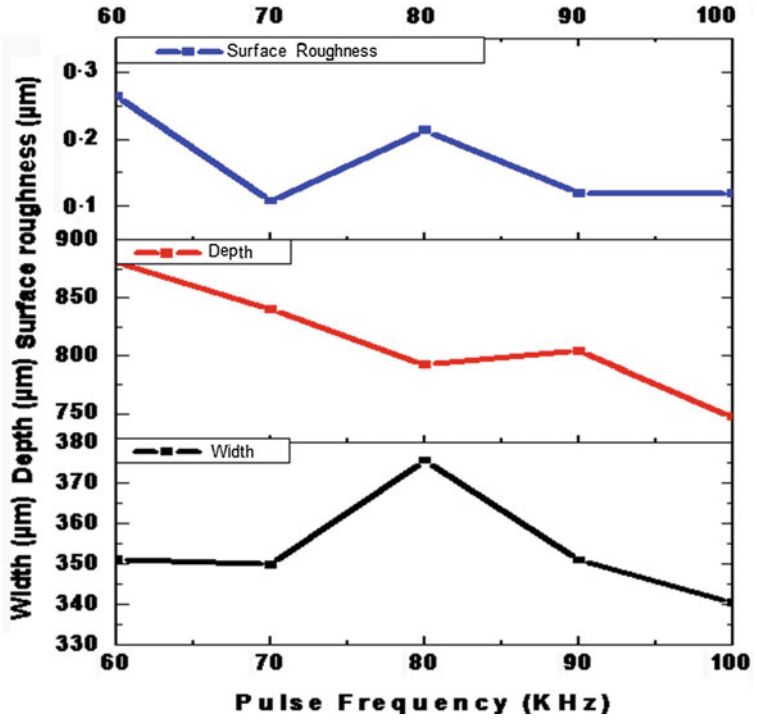

Fig. 5 Effect of pulse frequency on width, depth and surface roughness

process parameters constant, laser beam energy reduced inversely. This phenomenon holds true with the moderate high settings of scan speed. In contrast, this phenomenon reverts back with the combination of moderately low settings of scan speed with increased pulse frequency. Low settings of pulse frequency lead to the increase in laser beam energy. This causes more heat input to the micro-groove surface and thus melting of more amount of material was observed. Therefore, width and depth dimensions were relatively at high values in low pulse frequency. This phenomenon also holds true for producing rough micro-groove surfaces at low pulse frequency. In contrast, with the increase of pulse frequency with moderate high settings of number of passes, reduction of laser beam pulse energy as well as reduction of depth of penetration might occur. The effect of spot overlapping also has a pivotal role in micro-groove topology. In addition, the melted material may not be removed completely and the remaining melted material can be re-solidified at the micro-grooving edges at high settings of pulse frequency. Therefore, low heat generation at high settings of pulse frequency, led to moderate changes in the dimensions of both width and depth; even though a tendency to reduce in the dimensions of width and depth were observed. Along with this, reduction in surface roughness due to the low heat generation and more spot overlapping at these settings of pulse frequency was observed. Hence better micro-groove topology was produced with the increase of pulse frequency.

$$\text{Laser beam energy} = \frac{\text{Average power}}{\text{Pulse frequency}} \tag{1}$$

3.4.3 Influence of Number of Pass on Width, Depth and Surface Roughness on Ti-6Al-4V Micro-grooves

Figure 6 shows the influence of number of pass on width, depth and surface roughness of fiber laser machined micro-groove surfaces while other process parameters were kept constant as scan speed of 40 mm/s, pulse frequency of 50 kHz and average power of 30 W. The present parametric combinations of 12 set of experiments revealed that the experiments were carried out at high heat input on the micro-groove surfaces. It can be observed from Fig. 6 that the width increases with the number of passes, but reverts back after a certain increment of number of passes. This phenomenon happened due to the striking of laser beam on the work-piece surface in a repetitive manner during pulse on time. In addition, the length of focus was altered every time as the number of passes went on increasing. As a result of that spot size of the laser beam was increased significantly. Therefore, with the increased spot size, the penetration rate into the desired thickness of the work-piece

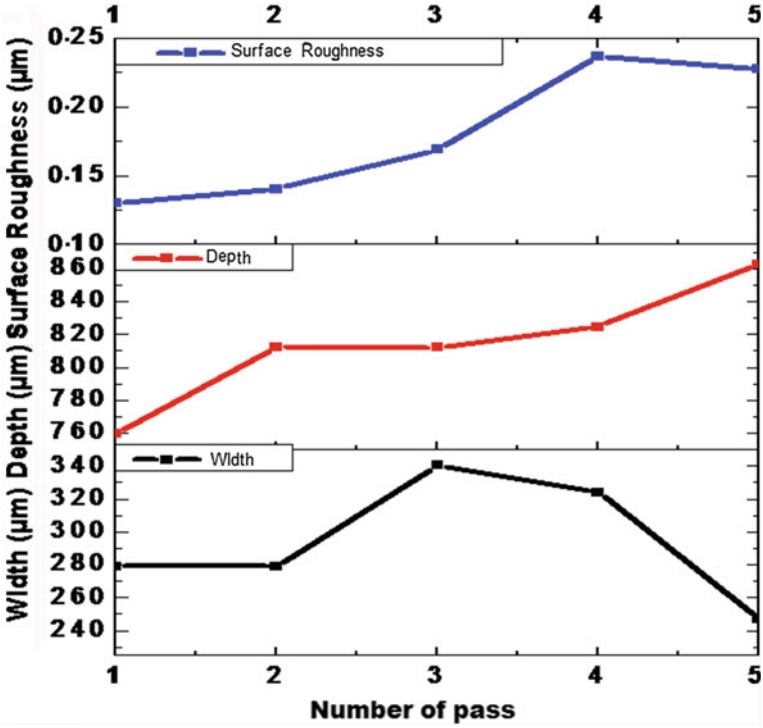

Fig. 6 Effect of number of pass on width, depth and surface roughness

could not be achieved. Due to repetitive striking of laser beam on the work-piece surface and pulse mode operation of fiber laser system, the depth increased. Due to the absence of inert gaseous systems in the present machining setup, some amount of molten material were re-solidified on the side wall of the micro-grooves. The moderate high setting of scan speed led to the phenomenon of sputtering at the edges of the micro-groove surfaces. Therefore, due to the combined effect of sputtering and re-solidification, the dimensions of width were reduced after certain increment of the number of passes as observed in Fig. 6. This phenomenon also holds true for micro-groove topology. The machined micro-grooves surfaces were rough as compared to those produced at low number of passes.

3.4.4 Influence of Average Power on Width, Depth and Surface Roughness

Laser power determines the direct energy input to the micro-cutting process. At lower laser powers, the energy supplied to the cutting front may be insufficient to cut through the desired depth of the material, whereas at higher powers, production

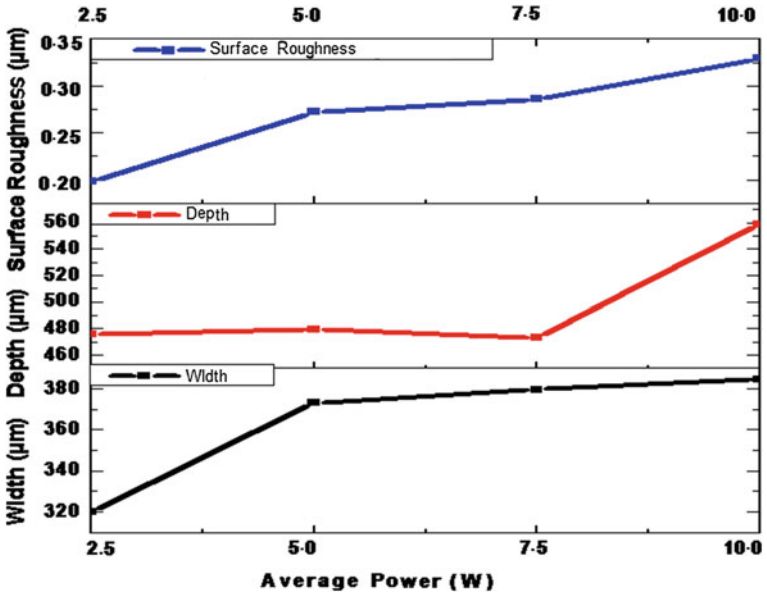

Fig. 7 Effect of average power on width, depth and surface roughness

of clean through cuts necessitates the reduction of cutting speed (Brown and Arnold 2010). Laser average power also determines the maximum cutting speed which is defined as the minimum speed at which through cut is produced. Both micro-cutting quality and performance is dependent on the laser average power.

Figure 7 represents the influence of the average power on width, depth and surface roughness of fiber laser machined micro-groove surfaces while other process parameters were kept constant such as 5 number of passes, scan speed of 100 mm/s and pulse frequency of 50 kHz. It can be observed from Fig. 7 that the amount of re-solidified material on the micro-groove surface increased with the increase in laser average power. Increase in laser power led to increase in the dimension of width up to a certain extent due to the increase in more power density and power input per unit area (refer to Eq. 1). In addition to this, low settings of pulse frequency produced more spot overlapping, continuos power density at the time of fiber laser micro-machining of Ti-6Al-4V micro-grooves. Hence, better micro-groove topologies were observed at low average power and vice versa. It was observed that the effect of laser energy in the geometry of the micro-grooves was not having the same functional dependence in both width and depth dimensions. The tendency of width dimensions was found to be increasing with the combine

parametric effects of low laser average power, low pulse frequency and high scan speed. Large heat input led to the removal of more amount of molten material from the micro-groove surfaces, although the peak power was moderately low due to high setting of pulse width. Hence, dimensions of groove depths were changed insignificantly with the increment of average power. The same can be stated in case of width dimensions which increased moderately up to a certain extent and then remained almost constant after that. It was also obvious that the focal plane varied each time during pulse off/on time and the rate ofpenetration also reduced as the machining time increased. Therefore, changes in the dimensions of both width and depth were insignificant.

3.5 Photographic Exhibits of Ti-6Al-4V Micro-grooves and Its Surface Characteristics

Figure 8a shows the micro-groove profiles of two micro-grooves measured in Leica 5× lens when scan speed was at 1000 and 900 mm/s respectively. Figure 8b and c shows the two micro-groove profiles of the width dimensions at different parametric settings i.e. 30 W of average power, scan speed of 40 mm/s, 4 number of passes and pulse frequency of 50 kHz and 30W of average power, scan speed of 40 mm/s, 8 number of passes and pulse frequency of 50 kHz respectively. Better micro-groove profile and reduction in width dimensions were observed when the number of passes was 8 as compare to number of passes were 4. Figure 9a, b provides the 3D view of four graphical displays of the measured data and other elements at different parametric settings as shown in the figures. At the right side of the 3D graphs, there is a color scale that shows which measured signal level that is mapped by the respective color. Therefore, Z height data is encoded with that colour scale and displayed 2-dimensionally. From Fig. 9a, it can be understood that when scan speed is 700 mm/s at 80 kHz of pulse frequency as compared to the scan speed of 40 mm/s at 60 kHz of pulse frequency, better finished micro-groove surfaces can be obtained. It can also be also observed that from Fig. 9b that at 12.5 W of laser average power (other parameters were constant) better surface topology can be obtained compared to average power of 30 W (other parameters were constant).Thus, selecting a combination of optimum parameters can lead to a better surface quality for potential application in the field of bio-medical engineering.

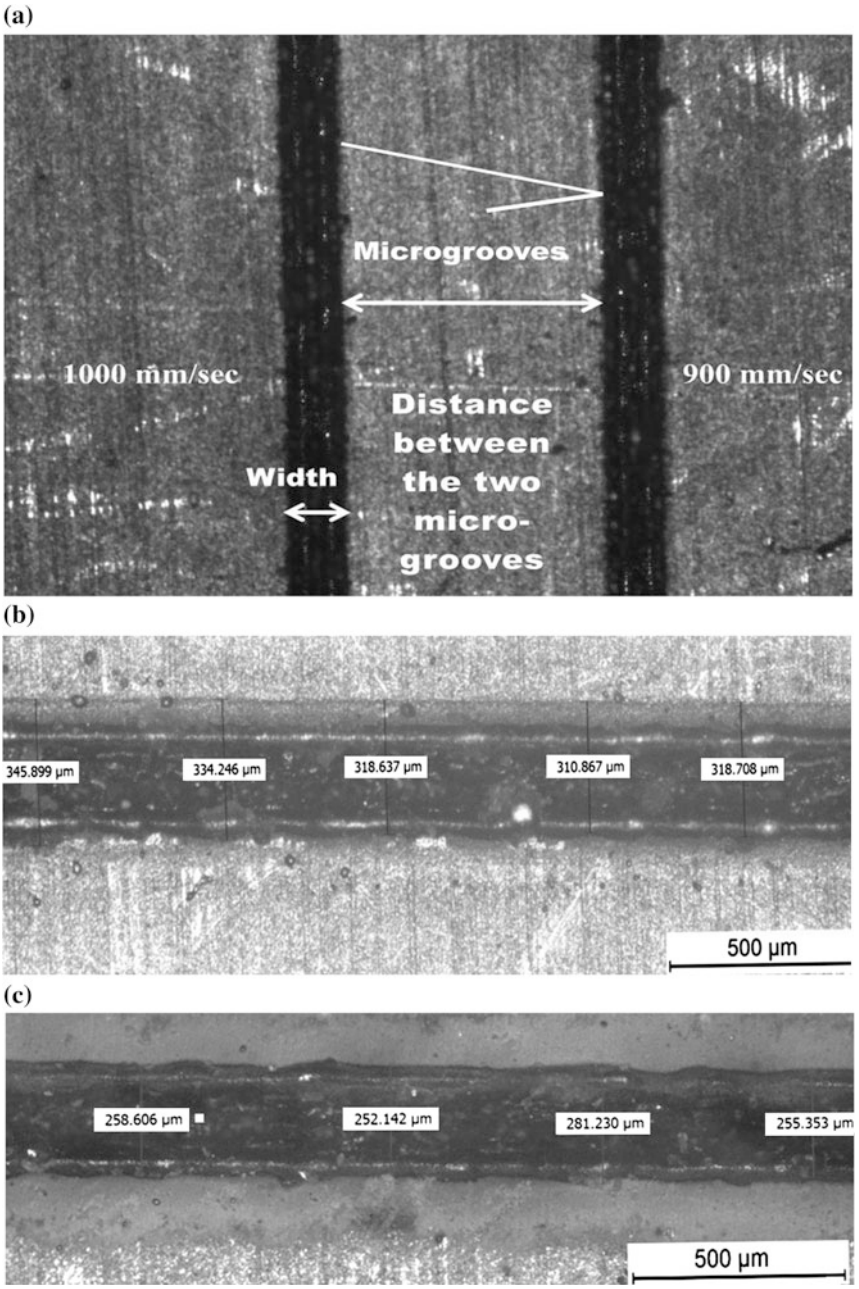

Fig. 8 **a** Microscopic view of different micro-groove profile at different scan speed. **b** and **c** Microscopic view of the micro-groove width at different number of passes

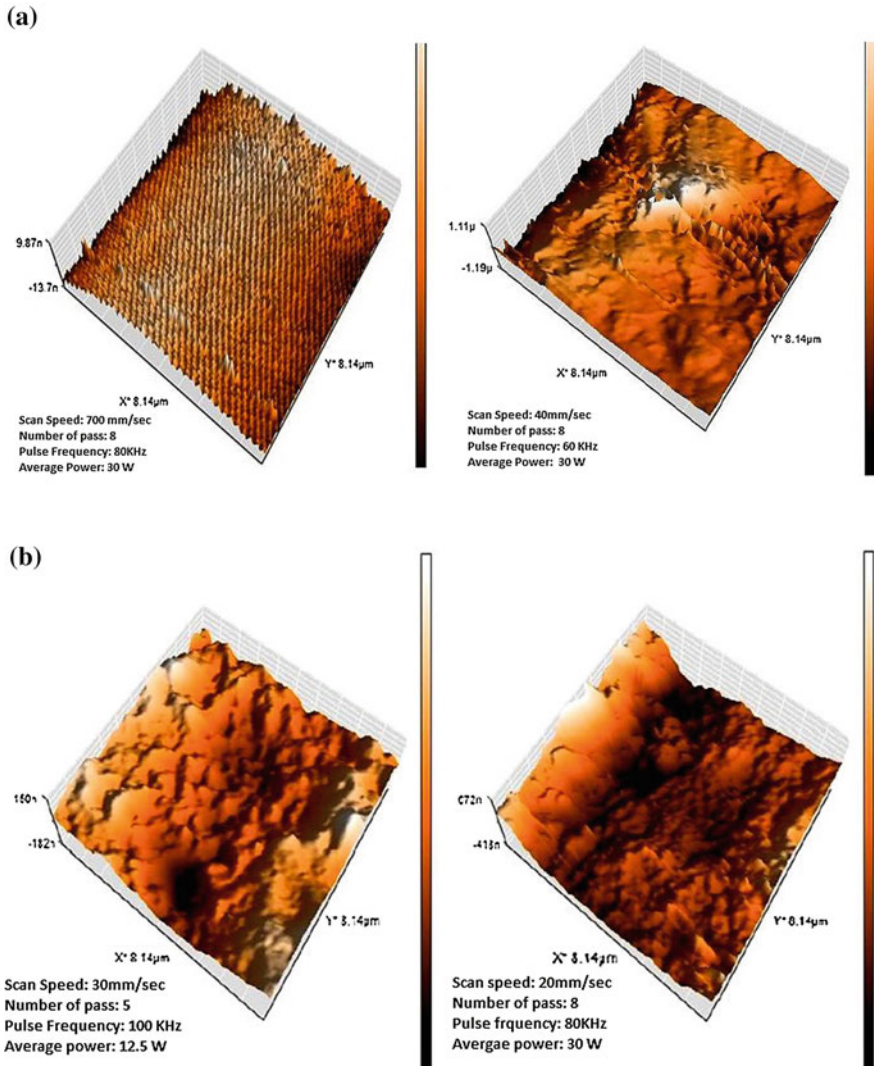

Fig. 9 **a**, **b** 3D representation of surface topology of the micro-grooved surface topologies at different parametric settings

4 Conclusions

Fiber laser micro-machining has a great potential for generating micro-grooves on Ti-6Al-4V. The present chapter mainly deals with the influence of four process parameters such as average power (2.5–30 W), number of passes (1–8), scan speed (40– 1000 mm/s), pulse frequency (50–100 kHz) during laser micro-grooving on

Ti-6Al-4V using 50 W diode pumped fiber laser. Different process parametric setting led to different width, depth and surface roughness. From the results of present experimentation, the following conclusions can be drawn.

(a) Depth and width dimensions tend to decrease with high scan speed with the combination of low pulse frequency, but surface roughness has a tendency to gradually increase owing to low spot overlapping and discontinuous power density at high scan speed.
(b) With the increase of pulse frequency combining moderate scan speed, reduction in the dimensions of width and depth can be observed owing to low heat generation. At higher values of pulse frequency, the more spot overlapping results continuous power density and smoother micro-groove surfaces.
(c) With the increment of number of pass, depth tends to increase while width decreases. After a certain number of pass, width will tend to decrease owing to re-solidification and sputtering of the molten material on the micro-grooved surface. Rough surface quality is observed due to the increase in the number of passes.
(d) As the average power increases, width and depth simultaneously increase due to more heat input and evaporate more amount of material from the micro-groove zone. Poor surface quality can also be observed with the increase of average power.

Fiber laser micro-machining is a unique process which can produce micro-grooves on titanium alloys with better accuracy. The growth of the fiber laser is commendable within a short span of time both in research and industrial perspectives. The present research work not only facilitates the use of fiber laser in the domain of micro-machining but also simplifies the complex phenomena of the micro-machining of the titanium alloys. Further research work can be carried out for determining parametric settings so as to achieve optimized values of better micro-machining quality along with minimum width and maximum depth.

Acknowledgments The authors acknowledge the financial support and assistance provided by CAS Ph-IV program of Production Engineering Department of Jadavpur University under University Grants Commission, New Delhi and TEQIP phase II program of Jadavpur University also M/S Sahajanand Laser Technology Limited for extending the machining facilities.

References

Al-Hajri, E., Ohadi, M., Dessiatoun, S. V., & Qi, J. (2005). Thermal performance of micro-structured evaporation surfaces: application to cooling of high flux microelectronics. *ASME Heat Transfer Division of Publication HTD, 376*, 799–805.

Almeida, I. A., Rossi, W. D., Lima, M. S. F., Berretta, J. R., Nogueira, G. E. C., Wetter, N. U., & Vieira, N. D, Jr. (2006). Optimization of titanium cutting by factorial analysis of the pulsed Nd: YAG laser parameters. *Journal of Materials Processing Technology, 179*, 105–110.

Brown, M. S., & Arnold, C. B. (2010). *Fundamentals of laser-material interaction and application to multiscale surface modification. Laser precision microfabrication*. Berlin: Springer.

Chen, J., Ulerich, J. P., Abelev, E., Fasasi, A., Arnold, C. B., & Soboyejo, W. O. (2009). An investigation of the initial attachment and orientation of osteoblast-like cells on laser grooved Ti-6Al-4V surfaces. *Materials Science and Engineering: C, 5*, 1442–1452.

Chesnutt, J., Thompson, A. W., & Williams, J. C. (1980). *Titanium 80. Science and technology* (pp. 1875). New York: AIME.

Collings, E. W. (1984). *The physical metallurgy of titanium alloys*. New York: American Society for Metals.

Dahotre, N. B., & Harimkar, S. P. (2008). *Laser fabrication and machining of materials*. New York: Springer.

Dandekar, C. R., Shin, Y. C., & Barnes, J. (2010). Machinability improvement of titanium alloy (Ti–6Al–4V) via LAM and hybrid machining. *International Journal of Machine Tools and Manufacture, 50*, 174–182.

Dhupal, D., Doloi, B., & Bhattacharyya, B. (2008). Pulsed Nd-YAG laser turning of micro-groove on aluminum oxide ceramic (Al_2O_3). *International Journal of Machine Tools and Manufacture, 48*, 236–248.

Ezugwu, E. O., Bonney, J., & Yamane, Y. (2003). An overview of the machinability of aeroengine alloys. *Journal of Materials Processing Technology, 134*, 233–253.

Fasasi, A. Y., Mwenifumbo, S., Rahbar, N., Chen, J., Li, M., Beye, A. C., et al. (2009). Nano-second UV laser processed micro-grooves on Ti6Al4V for biomedical applications. *Materials Science and Engineering C, 29*, 5–13.

Hayes, W. C., & Mow, V. C. (1997). *Basic orthopaedic biomechanics*. Philadelphia: Lippincott-Raven.

Hecht, J. (2009). Half a century of laser weapons. *Optics Photonics News, 20*, 16–21.

Hegarty, J., Broer, M. M., Golding, B., Simpson, J. R., & MacChesney, J. B. (1983). Photon echoes below 1 K in a Nd^{3+}-doped glass fiber. *Physics Revised Letter, 51*, 2033–2035.

Koester, C. J., & Snitzer, E. (1964). Amplification in a fiber laser. *Applied Optics, 3*, 1182.

Mahrle, A., & Beyer, E. (2009). Theoretical aspects of fiber laser cutting. *Journal of Physics D: Applied Physics, 42*, 175507 (9 pp.).

Masuzawa, T., & Tonshoff, H. K. (1997). Three-dimensional micromachining by machine tools. *Annuals of the CIRP, 46*, 621–628.

Mauclair, C., Landon, S., Pietroy, D., Baubeau, E., Stoian, R., & Audouard, E. (2013). Ultrafast laser machining of micro grooves on stainless steel with spatially optimized intensity distribution. *JLMN-Journal of Laser Micro/Nano Engineering, 8*, 11.

Meijer, J. (2002). *Laser micromachining, micromachining of engineering materials*. USA: Marcel Dekker.

Nakazawa, M., Kimura, Y., & Suzuki, K. (1989). Efficient Er^{3+}-doped optical fiber amplifier pumped by a 1.48 μm InGasP laser diode. *Applied Physics Letter*, *54*, 295−297.

Olsen, F. O., Hansen, K. S., & Nielsen, J. S. (2009). Multibeam fiber laser cutting. *Journal of Laser Applications, 21*, 133.

Poole, S. B., Payne, D. N., & Fermann, M. E. (1985). Fabrication of low loss optical fibers containing rare earth ions. *Electronics Letter, 21*, 737–773.

Rashid, R. A. R., Sun, S., Wang, G., & Dargusch, M. S. (2012). An investigation of cutting forces and cutting temperatures during laser-assisted machining of the Ti–6Cr–5Mo–5V–4Al beta titanium alloy. *International Journal of Machine Tools and Manufacture, 63*, 58–69.

Rathod, V., Doloi, B., & Bhattacharyya, B. (2013). Influence of electrochemical micromachining parameters during generation of micro-grooves. *The International Journal of Advanced Manufacturing Technology,*. doi:10.1007/s00170-013-5304-3.

Ratner, B. D., Hoffman, A. S., Schoen, F. J., & Lemons, J. E. (1996). *An introduction to materials in medicine, biomaterials science*. San Diego: Academic Press.

Schaeffer, R. D. (2012). *Fundamentals of laser micro-machining*. Boca Raton: CRC Press-Taylor & Francis Group.

Shelton, J. A., & Shin, Y. C. (2010a). Experimental evaluation of laser-assisted micromilling in a slotting configuration. *Journal of Manufacturing Science and Engineering, Transactions of the ASME, 132*, 0210081.

Shelton, J. A., & Shin, Y. C. (2010b). Comparative evaluation of laser-assisted micromilling for AISI 316, AISI 422, Ti–6Al–4V and inconel 718 in a side-cutting configuration. *Journal of Micromechanics and Micro engineering, 20*, 075012.

Sieniawski, J., Ziaja, W., Kubiak, K., & Motyka, M. (2013). *Microstructure and mechanical properties of high strength two-phase titanium alloys, titanium alloys—advances in properties control*. Croatia: In Tech.

Snitzer, E. (1961). Proposed fiber cavities for optical masers. *Journal of Applied Physics, 23*, 36–39.

Steen, W., & Mazumder, J. (2010). *Laser material processing*. London: Springer.

Sun, S., & Brandt, M. (2013). *Laser beam machining, nontraditional machining processes*. London: Springer.

Sun, S., Brandt, M., Barnes, J. E., & Dargusch, M. S. (2011). Experimental investigation of cutting forces and tool wear during laser-assisted milling of Ti–6Al–4V alloy. *Proceedings of the Institution of Mechanical Engineers, Part B: Journal of Engineering Manufacture, 225*, 1512–1527.

Sun, S. J., Harris, J., & Brandt, M. (2008). Parametric investigation of laser-assisted machining of commercially pure titanium. *Advanced Engineering Materials, 10*, 565–572.

Teodoro, F. D. (2011). *Pulsed fiber laser, high power laser hand book*. New York, USA: McGraw-Hill.

Tian, Y., Wu, B., Anderson, M., & Shin, Y. C. (2008). Laser-assisted milling of silicon nitride ceramics and Inconel 718. *Journal of Manufacturing Science and Engineering, Transactions of the ASME, 130*, 031013.

Wang, W., & Poh, C. K. (2013). *Titanium alloys in orthopaedics, titanium alloys—advances in properties control*. Croatia: In Tech.

Williams, D.F. (1984). *Titanium and titanium alloys, biocompatibility of clinical implant materials* (pp. 44–47). Boca Raton: CRC Press-Taylor & Fransis.

Yang, J., Sun, S., Brandt, M., & Yan, W. (2010). Experimental investigation and 3D finite element prediction of the heat affected zone during laser assisted machining ofTi6Al4V alloy. *Journal of Materials Processing Technology, 210*, 2215–2222.

Zhang, S. Y., Lin, X., Chen, J., & Huang, W. D. (2007). Influence of heat treatment on the microstructure and properties of Ti–6Al–4V titanium alloy by laser rapid forming. *Rare Metal Materials and Engineering, 36*, 1263–1266.